Exp Brain Res
DOI 10.1007/s00221-017-5108-z

RESEARCH ARTICLE

The speed-curvature power law of movements: a reappraisal

Myrka Zago[1] · Adam Matic[2] · Tamar Flash[3] · Alex Gomez-Marin[2] · Francesco Lacquaniti[1,4,5]

Received: 26 July 2017 / Accepted: 13 October 2017

Abstract Several types of curvilinear movements obey approximately the so called 2/3 power law, according to which the angular speed varies proportionally to the 2/3 power of the curvature. The origin of the law is debated but it is generally thought to depend on physiological mechanisms. However, a recent paper (Marken and Shaffer, Exp Brain Res 88:685–690, 2017) claims that this power law is simply a statistical artifact, being a mathematical consequence of the way speed and curvature are calculated. Here we reject this hypothesis by showing that the speed-curvature power law of biological movements is non-trivial. First, we confirm that the power exponent varies with the shape of human drawing movements and with environmental factors. Second, we report experimental data from *Drosophila larvae* demonstrating that the power law does not depend on how curvature is calculated. Third, we prove that the law can be violated by means of several mathematical and physical examples. Finally, we discuss biological constraints that may underlie speed-curvature power laws discovered in empirical studies.

Keywords Motor control · Drawing · Two-thirds power law · Statistical analysis

Introduction

One of the best-studied characteristics of human voluntary movements is the empirical relationship between instantaneous speed and local path curvature. Speed—distance divided by time—is a spatio-temporal property of movement, while curvature is a purely spatial property, corresponding to the extent to which the trajectory bends relative to a straight line. Although a given trajectory can be traced with infinitely many different speed profiles, biological constraints restrict the degrees of freedom with the result that speed generally co-varies with curvature throughout a given continuous movement (Viviani and Terzuolo 1982). Specifically, in a planar drawing of elliptic shapes, the angular speed of the pen tip varies in close proportion to the 2/3 power of the curvature of the trace (so called 2/3 power law, Lacquaniti et al. 1983).

Since the original demonstration, the 2/3 power law has been largely confirmed for elliptic trajectories drawn in 2D space (Viviani and Schneider 1991; Viviani and Flash 1995; Richardson and Flash 2002; Flash and Handzel 2007; Huh and Sejnowski 2015; Catavitello et al. 2016) or 3D space (Soechting and Terzuolo 1986; Flanders et al. 2006; Maoz et al. 2009). Moreover, speed-curvature power relationships have been reported for many other types of movements, including isometric 3D force trajectories (Massey et al. 1992), walking trajectories (Vieilledent et al. 2001; Ivanenko et al. 2002; Hicheur et al. 2005), and smooth pursuit eye

Myrka Zago and Adam Matic contributed equally to the work.

✉ Francesco Lacquaniti
lacquaniti@med.uniroma2.it

[1] Laboratory of Neuromotor Physiology, IRCCS Santa Lucia Foundation, Via Ardeatina 306, 00179 Rome, Italy

[2] Behavior of Organisms Laboratory, Instituto de Neurociencias CSIC-UMH, Av Ramón y Cajal, Alicante, Spain

[3] Department of Applied Mathematics and Computer Science, Weizmann Institute of Science, Rehovot 76100, Israel

[4] Department of Systems Medicine, Medical School, University of Rome Tor Vergata, Via Montpellier 1, 00133 Rome, Italy

[5] Centre of Space Bio-medicine, University of Rome Tor Vergata, Via Montpellier 1, 00133 Rome, Italy

Published online: 25 October 2017

movements (de'Sperati and Viviani 1997). Deviations from the 2/3 value of the exponent occur at inflection points of the trajectory where the prescribed tangential speed would become infinite, but they also occur for some trajectories without inflection points, such as ellipses with low eccentricities or large sizes (Wann et al. 1988; Schaal and Sternad 2001), or other shapes (Massey et al. 1992; Schaal and Sternad 2001; Richardson and Flash 2002; Dounskaia 2007; Flash and Handzel 2007; Bennequin et al. 2009; Huh and Sejnowski 2015).

The power law has been studied mainly in humans, but it also applies to drawings made by monkeys (Schwartz 1994; Abeles et al. 2013) and to crawling movements of Drosophila larvae (Zago et al. 2016). Thus, the power law might be a recurrent law underlying several biological movements. It is generally thought to depend on physiological mechanisms, although its exact origin remains debated. In particular, it has been suggested that the law might be due to kinematic or dynamic constraints arising at some level of the neuro-musculo-skeletal chain (Schwartz 1994; Viviani and Flash 1995; Gribble and Ostry 1996; Harris and Wolpert 1998; Schaal and Sternad 2001; Dounskaia 2007; Flash and Handzel 2007; Bennequin et al. 2009; Polyakov et al. 2009; Huh and Sejnowski 2015; Zago et al. 2016).

Now, a paper recently published in this journal (Marken and Shaffer 2017, in the following abbreviated as M/S) claims that the 2/3 power law is just an artifact, being a mathematical consequence of the way the critical variables of speed and curvature are calculated. If true, the contention put forth by M/S would have a significant impact on the field of motor control, since the power law is often considered as one of the hallmarks of curvilinear movements (e.g., Wolpert et al. 2013).

Here we reassess the validity of the speed-curvature power law by considering previous work as well as new data. In particular, we show that (a) the power law is not a trivial relationship given by mathematics or physics, (b) it does not depend on the methods used to compute the critical variables, and (c) the exponent of the power law is not fixed to 2/3 but varies with the shape of movement and with environmental factors. Based on these points, we reject the hypothesis that the empirical power law is a mathematical or statistical artifact.

Basic notions on the geometry of curves

As remarked at the outset of this article, a priori any given path of movement can be traced with infinitely many speed profiles, since the path specifies the instantaneous movement direction but not the speed. Moreover, any path can be defined independently of the law of motion. Speed and path become jointly determined only when a specific kinematic law is provided.

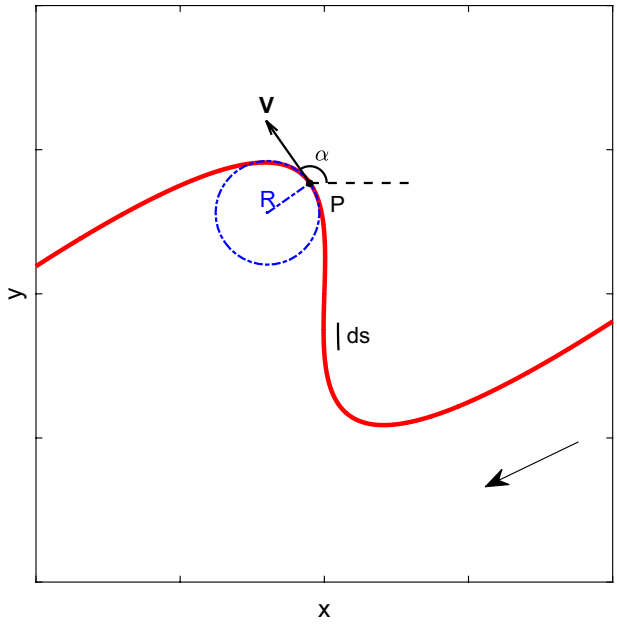

Fig. 1 Schematic illustration of kinematic and geometric variables for an arbitrary trajectory described by a moving point P (see text for details). $\mathbf{V}$ is the vector of tangential velocity, α the tangential angle, R the radius of curvature (radius of the osculating circle)

We first review the definitions of the critical variables from elementary differential geometry of planar, continuous, differentiable, regular curves (for 3D curves, see for example Struik 2012; Gielen et al. 2009; Pollick et al. 2009). The position of a point P moving along the curve (Fig. 1) can be described by the functions of time $x = f(t)$ and $y = g(t)$, as well as by the arc-length s along the curve measured from a starting point (x_0, y_0). Then, given unit vectors $\mathbf{i}$[1] and $\mathbf{j}$ along the x and y axis, respectively, the vector from the origin to P is $\mathbf{R} = \mathbf{i}x + \mathbf{j}y = \mathbf{i}f(t) + \mathbf{j}g(t) = \mathbf{R}(s)$, the tangential velocity vector is $\mathbf{V} = \frac{\mathrm{d}\mathbf{R}}{\mathrm{d}t} = \mathbf{i}\frac{\mathrm{d}x}{\mathrm{d}t} + \mathbf{j}\frac{\mathrm{d}y}{\mathrm{d}t}$, with magnitude (speed[2]) $V = |\mathbf{V}| = \left|\frac{\mathrm{d}\mathbf{R}}{\mathrm{d}t}\right| = \sqrt{\left(\frac{\mathrm{d}x}{\mathrm{d}t}\right)^2 + \left(\frac{\mathrm{d}y}{\mathrm{d}t}\right)^2} = \left|\frac{\mathrm{d}s}{\mathrm{d}t}\right|$. We can associate to P a moving frame (Frenet-Serret frame) composed of tangent and normal unit vectors, $\mathbf{T}$ and $\mathbf{N}$ respectively. $\mathbf{T} = \frac{\mathrm{d}\mathbf{R}}{\mathrm{d}s} = \mathbf{i}\frac{\mathrm{d}x}{\mathrm{d}s} + \mathbf{j}\frac{\mathrm{d}y}{\mathrm{d}s} = \frac{\mathbf{V}}{|\mathbf{V}|}$, $\mathbf{N} = \frac{\mathrm{d}\mathbf{T}/\mathrm{d}s}{|\mathrm{d}\mathbf{T}/\mathrm{d}s|}$. Thus, $\mathbf{V} = \mathbf{T}|\mathbf{V}|$ and $\mathbf{V} = \boldsymbol{\Omega} \times \mathbf{R}$ where $\boldsymbol{\Omega}$ is the vector of angular velocity. We can measure the direction of $\mathbf{T}$ by means of the tangential angle α, that is, the angle between the tangent line to the

[1] Bold characters denote vector quantities throughout.

[2] Although the terms velocity and speed are often used interchangeably in the literature (including M/S), the former denotes the vector with a magnitude and direction while the latter denotes the magnitude only.

curve at the given point and the x-axis. Angular speed (magnitude of angular velocity vector) corresponds to the absolute value of the rate of change of α with respect to time $A = |\mathbf{\Omega}| = \left|\frac{d\alpha}{dt}\right|$. Curvature C corresponds to the absolute value of the rate of change of α with respect to arc-length $C = \left|\frac{d\alpha}{ds}\right| = \left|\frac{d\mathbf{T}}{ds}\right| = \left|\frac{d^2\mathbf{R}}{ds^2}\right|$, and $C\mathbf{N} = \frac{d\mathbf{T}}{ds}$. Radius of curvature R is the inverse of C and corresponds to the radius of the osculating circle, i.e., the circle passing through the point P and two other points on the curve infinitesimally close to P.

From the above equations $V = \left|\frac{ds}{dt}\right|$, $A = \left|\frac{d\alpha}{dt}\right|$, $C = \left|\frac{d\alpha}{ds}\right|$, it can be seen that speed (whether tangential or angular) is independent of curvature (or radius of curvature) in the absence of constraints. In other words, the curvature profile uniquely specifies the shape of a movement, independently of the speed profile (Bennequin et al. 2009; Huh and Sejnowski 2015).

Empirical speed-curvature power laws for human drawing have different exponents

As is the case for all biological power laws (West 2017), also the speed-curvature power law is an approximation. Most previous studies investigating speed-curvature relationships in biological movements tested the hypothesis that angular speed A is approximately proportional to curvature C raised to an exponent β:

$$A \approx KC^{\beta} \tag{1}$$

where A and C are measured at each instant of time at the endpoint that traces the trajectory (the pen tip for hand-drawing). A different but mathematically equivalent formulation of speed-curvature relationships involves V instead of A, and R instead of C. Because $A = V/R$ and $R = 1/C$, Eq. 1 is equivalent to:

$$V \approx KC^{-(1-\beta)} = KR^{(1-\beta)} \tag{2}$$

The relationships of Eqs. 1–2 can also be expressed using logarithms, yielding respectively:

$$\log A \approx \log K + \beta \log C \tag{3}$$

$$\log V \approx \log K + (1-\beta) \log R \tag{4}$$

In the case of normal hand-drawing of ellipses, the exponent β is approximately equal to 2/3 and K is roughly constant throughout the drawing, being related to the overall tempo of the movement and increasing proportionally to the average speed (Lacquaniti et al. 1983). For more complex trajectories such as the scribbles, K is piecewise constant (Lacquaniti et al. 1983, 1984; Viviani and Cenzato 1985; Richardson and Flash 2002).

In general, however, the power exponent β is not invariant. Dynamic factors may affect its value (Wann et al. 1988; Gribble and Ostry 1996), as shown by a recent study comparing elliptic drawing movements performed in air and water at the same average speed (Catavitello et al. 2016). The speed-curvature law held in both conditions, but the exponent was close to 2/3 in air and 3/4 in water, indicating that the speed-curvature coupling is affected by the viscosity of the medium where the movement unfolds.

A major factor affecting the specific value of the exponent β is determined by the shape of the drawn trajectory. Thus, deviations from the 2/3 value of the exponent were noticed for specific curves such as the asymmetrical lemniscate (Viviani and Flash 1995; Richardson and Flash 2002; Flash and Handzel 2007). Several models based on the optimization of different kinematic costs (Richardson and Flash 2002, Huh and Sejnowski 2015) or on assuming non-Euclidean geometrical representations of movements (Flash and Handzel 2007; Bennequin et al. 2009; Polyakov et al. 2009) were developed to account for such deviations. A thorough investigation of the shape dependency of the exponent has recently been carried out by Huh and Sejnowski (2015). They considered a wide set of planar convex curves that differ in terms of the spatial angular frequency (Huh 2015). Angular frequency ν of a curve is the number of curvature oscillations per cycle. For instance, ν is equal to 2 for an ellipse, because the curvature profile fluctuates twice per cycle. At integer frequencies $\nu > 2$, the curves resemble rounded regular polygons. In general, a convex curve with a rational frequency $\nu = m/n$, where m and n are coprime integers (i.e., no common factors) and $m \neq 1$, has a closed shape of period $2\pi n$, and exhibits m degrees of rotational symmetry. For such pure frequency curves, Huh and Sejnowski (2015) described a spectrum of power laws with exponents covering a wide range. The exponent of the angular speed-curvature power law ranged from about 0.34 for a curve with $\nu = 2/33$ up to about 0.90 for a curve with $\nu = 6$, and including an exponent of 0.65 for the ellipse ($\nu = 2$), close to the value reported in previous studies for the latter curve.

The finding that drawing different shapes results in very different values of the power exponent is important because it reveals potential physiological mechanisms underlying movement generation (see section Biological constraints on speed-curvature relationships). Given the relevance of this issue for the present discussion, here we replicated part of the protocol by Huh and Sejnowski (2015) to verify the strong shape-dependency of the power exponent.

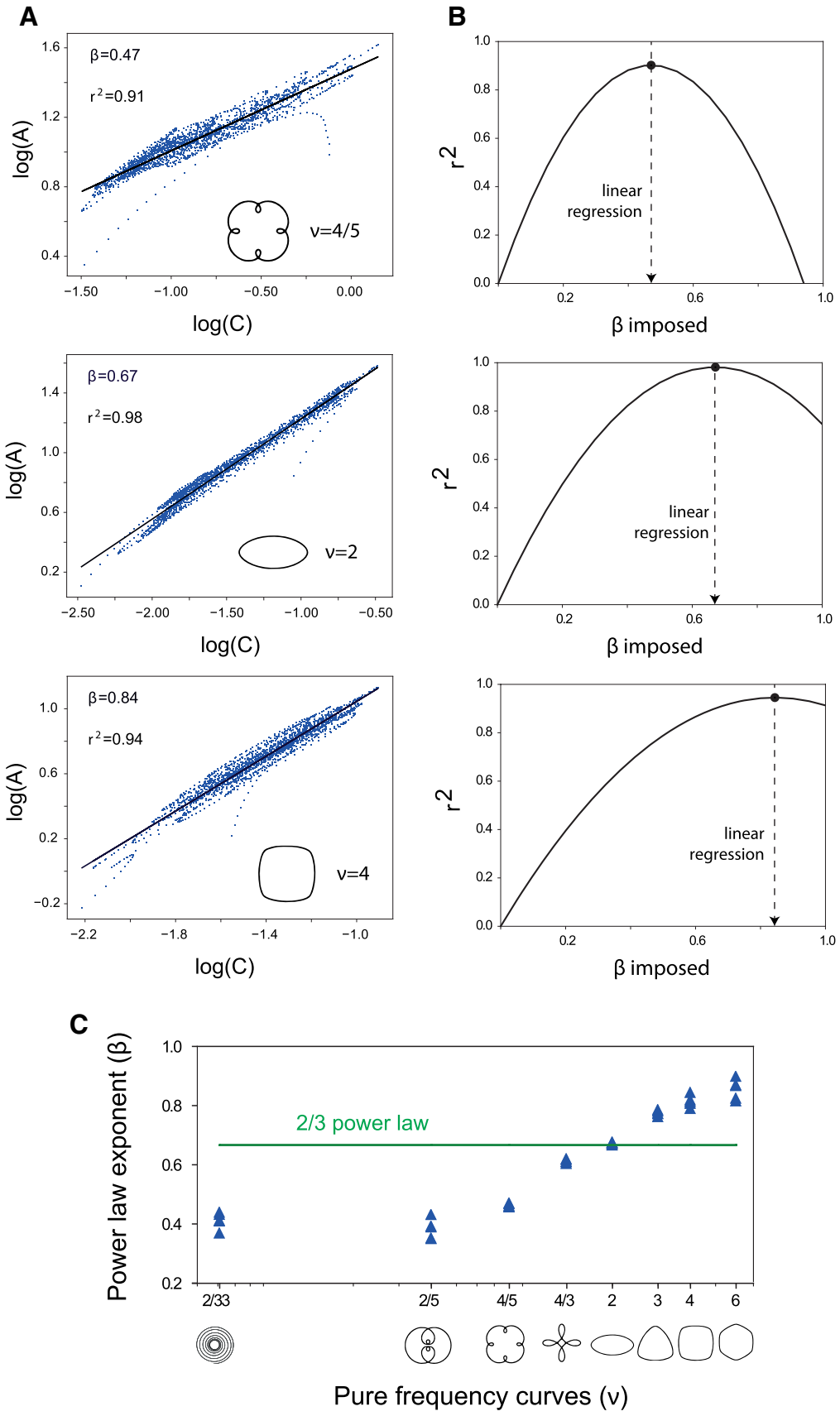
A
β=0.47
r²=0.91
log(A)
log(C)
ν=4/5
β=0.67
r²=0.98
ν=2
β=0.84
r²=0.94
ν=4
B
r2
linear
regression
β imposed
C
Power law exponent (β)
2/3 power law
2/33
2/5
4/5
4/3
2
3
4
6
Pure frequency curves (ν)

◂**Fig. 2** Dependence of the power exponent on the shape of human drawings. **a** Power laws for movement trajectories characterized by angular frequency (ν) equal to 4/5 (four-leaf), 2 (ellipse) and 4 (rounded square), from top to bottom. Scatter plots of instantaneous angular speed and curvature on log–log scale. The data were best-fitted (black line), with β-exponent and variance accounted for (r^2) as indicated in the insets. **b** Plots of r^2 resulting from imposing β-exponents in the range 0–1 in the power function for the corresponding drawings of panel (A). The best-fitting β-exponent is indicated by the vertical dashed line. **c** Best-fitting exponents (blue triangles) as a function of angular frequency (ν) of all eight drawn shapes

Methods and results

We used the same eight curves included in Fig. 5 of Huh and Sejnowski (2015). The angular frequency ν of these curves was 2/33, 2/5, 4/5, 4/3, 2, 3, 4, and 6. These curves (typical size 10 cm) were presented on a sheet of paper that was placed on top of a digitizing tablet (Wacom Intuos ProS PTH-451, spatial resolution: 0.08 mm, sampling rate: 200 samples/s). Three participants traced the curves continuously over 30 s with the tablet stylus (leaving no trace behind). They had previously given written informed consent to procedures approved by the Institutional Review Board, and had been instructed to draw with fast and fluid movements without corrections. The tempo of the movements (average speed) was indicated by a metronome with a period of 0.6 s. The x, y position-samples of the stylus tip were low-pass filtered (5 Hz cut-off, second-order, zero-phase-lag Butterworth filter), and interpolated using cubic splines to obtain the first and second time derivatives. Linear regressions of log A versus log C (Eq. 3) was used to estimate the exponent (β) of a power law $A = KC^{\beta}$. Here and throughout the article, log denotes base 10 logarithm ($\log_{10}$).

Figure 2a shows the results for three different curves. Data were well fitted by a power law, but the power exponent β systematically increased with the angular frequency of the curve, in agreement with Huh and Sejnowski (2015). Only for the ellipse did the exponent comply with the 2/3 power law, while for the other two curves the exponents deviated substantially from 2/3. Notice that the fit of the power relationships was quite sensitive to the specific value of β, as shown by forcing other β values (Fig. 2b).

Figure 2c shows the best-fitting exponents for all eight drawn shapes plotted as a function of the respective angular frequency (ν). Again in agreement with Huh and Sejnowski (2015), the overall β versus ν relationship was S-shaped. The variance accounted for (r^2) by the log–log linear regressions in each trial of each curve was greater than 0.83 ($\nu = 6$), 0.86 ($\nu = 4$), 0.93 ($\nu = 3$), 0.97 ($\nu = 2$), 0.94 ($\nu = 4/3$), 0.87 ($\nu = 4/5$), 0.72 ($\nu = 2/5$) and 0.55 ($\nu = 2/33$). Participants had some difficulty to trace accurately the curves with very high or very low angular frequencies, and the log–log regressions fitted the data less well than those at intermediate frequencies, as also reported in Huh and Sejnowski (2015).

In sum, the present results confirm the strong shape dependency of the exponent of the speed-curvature power law, consistent with Bennequin et al. (2009) and Huh and Sejnowski (2015).

Empirical power laws do not depend on how curvature is computed

Although speed and curvature are mathematically independent (see above), in practice some spurious correlation between the two measured variables might result from the time discretization due to a finite sampling rate and from using temporal derivatives in the calculation of both speed and curvature. In other words, the time-sampled spatial coordinates used to estimate local curvature might reflect to some extent also the speed of movement. This can be seen by re-parametrizing curvature first with respect to x, y coordinates and then with respect to time. Thus, from $C = \left|\frac{d\alpha/dx}{ds/dx}\right| = \frac{|d^2y/dx^2|}{[1+dy/dx^2]^{3/2}} = \left|\frac{d\alpha/dt}{ds/dt}\right|$, $x = f(t)$ and $y = g(t)$, $\alpha = \tan^{-1}\left(\frac{dy/dt}{dx/dt}\right)$, we can derive $C = \frac{\left|\frac{dx}{dt}\frac{d^2y}{dt^2} - \frac{dy}{dt}\frac{d^2x}{dt^2}\right|}{\left[\frac{dx}{dt}^2 + \frac{dy}{dt}^2\right]^{3/2}}$ or using the dot notation for time derivatives.

$$C = \frac{|\dot{x}\ddot{y} - \ddot{x}\dot{y}|}{(\dot{x}^2 + \dot{y}^2)^{3/2}} \tag{5}$$

In this section, we compare empirical speed-curvature relationships for crawling larvae using different sampling rates and different methods to calculate path curvature. To this end, we re-analyzed data presented in Zago et al. (2016).

Methods and results

For details on the experimental procedures and tracking of larvae behavior, see Gomez-Marin et al. (2011, 2012) and Zago et al. (2016). All procedures were in accordance with the ethical standards of the institution at which the experimental recordings were performed. Briefly, *Drosophila melanogaster* larvae in the foraging stage crawled on a viscous medium and were tracked at 7 frames/s, 90 µm/pixel. These sampling parameters have been shown to be fully adequate for the slow, small movements of these animals (Gomez-Marin et al. 2011, 2012). Three groups of larvae were exposed to different sensory environments, resulting in three different types of crawling trajectories, overshoot ($n = 42$ larvae), approach ($n = 40$), and dispersal ($n = 41$). The x, y position-samples of the larvae centroid were low-pass filtered (0.07 Hz cut-off, second-order, zero-phase-lag Butterworth filter), and interpolated with cubic splines.

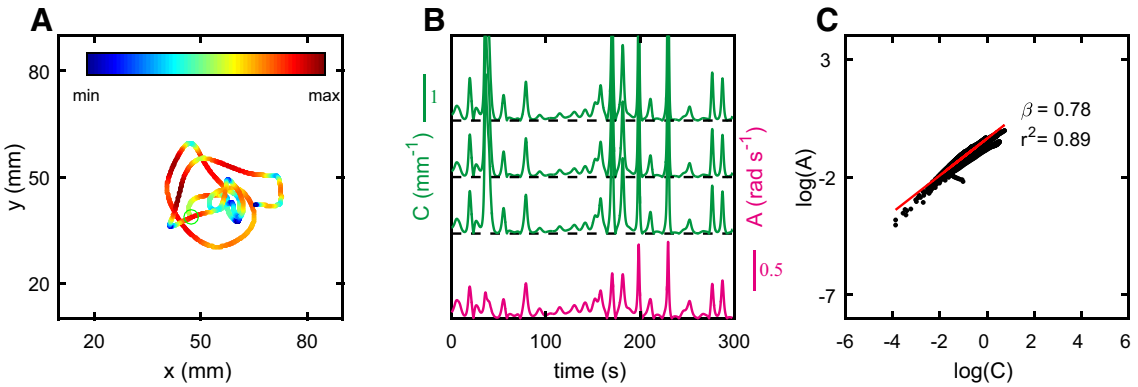

Fig. 3 Empirical relation between angular speed and curvature in a crawling larva. **a** Trajectory of the larva centroid. Green circle indicates starting position. Each point of the trajectory is colored according to the instantaneous tangential speed. **b** Time course of the angular speed (A, red) and curvature (C, green) for the trajectory plotted in panel A. The three traces of curvature are plotted with an offset between each other and correspond to curvature computed as in Eq. 5 (top), as the spatial derivative of the angle coordinate (middle), and as the inverse of the radius of the osculating circle (bottom). The dashed horizontal lines correspond to $C = 0$ in all three cases. **c** Scatter-plot of instantaneous angular speed A and curvature C on log–log scale. The data were best-fitted (red line) with β-exponent and variance accounted for (r^2) as indicated in the inset. These data refer to curvature computed according to method 1) above. In this example, β and r^2 values differed by $< 10^{-4}$ between the three methods

Curvature was then computed using three different methods: (1) as $C = \frac{|\dot{x}\ddot{y}-\ddot{x}\dot{y}|}{(\dot{x}^2+\dot{y}^2)^{3/2}}$ with the time parametrization (Eq. 5), (2) as the spatial derivative of the angle coordinate $C = \left|\frac{d\alpha}{ds}\right|$, (3) as the inverse of the radius of the osculating circle. Before computing $d\alpha/ds$ (method 2), we oversampled the original data by a factor 1000 (corresponding to a rate of 7000 samples/s) in order to dilute any time dependence of the spatial coordinates. To compute the osculating circle (method 3), we oversampled the data by a factor of 10, and then we best fitted a circle to any 3 consecutive x, y samples. Next, we performed least-squares orthogonal-regression of log angular speed A versus log curvature C (Eq. 3), the latter being computed with one of the three methods described above.

Figure 3a shows a typical trajectory traced by a crawling larva in the overshoot condition. These trajectories were not associated with a constant progression speed or any simple kinematic pattern. Both the instantaneous angular speed and the local path curvature were widely modulated, yet they co-varied throughout (Fig. 3b). Notice that the time profiles of curvature derived with the three methods described above are essentially identical (for clarity, they are plotted with an offset in Fig. 3b). A log–log plot of angular speed versus curvature revealed a power law as a straight line whose slope corresponds to the power-exponent β (Fig. 3c). We found no statistically significant difference in the linear regression parameters (slope β and r^2) between the results obtained with the three methods used to compute curvature (Kruskal–Wallis ANOVA by ranks followed by multiple comparisons, $P > 0.95$ in all three groups of larvae). The median value of β was 0.78 (interquartile-range = 0.06), 0.78 (interquartile-range = 0.08), and 0.76 (interquartile-range = 0.06) for the overshoot, approach, and dispersal conditions, respectively. The maximum difference between the slope β computed with one of the three methods and the slope computed with the other two methods was $< 0.1\%$ of the maximum value. Median value of r^2 was > 0.91 for all three methods.

These results show that the empirical speed-curvature relationships of the crawling larvae are very little affected by the specific method used to estimate path curvature, indicating that the numerical calculations typically used are unlikely to introduce any significant cross-talk between curvature estimates and speed estimates, irrespective of the specific parametrization.

A power exponent close to 3/4 in crawling larvae is reminiscent of the value found for human drawing movements in water (Catavitello et al. 2016), and thus it might depend on the viscosity of the medium (Zago et al. 2016). Alternatively, it could be attributed to the complex shape of the trajectories traced by the larvae. Irrespective of the origin, the deviation of the exponent from 2/3 reinforces the notion that the power exponent is not constant in biological movements.

Zago et al. (2016) also checked for the potential contamination of speed-curvature relationships by noise in the data (Maoz et al. 2006). Their Fig. S1 shows that the values of β and r^2 of the log–log regression of speed versus curvature depend little on the specific value of the low-pass frequency cut-off used to filter the position data of the crawling larvae.

A different way to look at speed-curvature relationships

Since $V = (\dot{x}^2 + \dot{y}^2)^{1/2} = A/C$ and $C = \frac{|\dot{x}\ddot{y} - \ddot{x}\dot{y}|}{(\dot{x}^2+\dot{y}^2)^{3/2}} = \frac{|\dot{x}\ddot{y} - \ddot{x}\dot{y}|}{V^3}$, by substitution we obtain $A = |\dot{x}\ddot{y} - \ddot{x}\dot{y}|^{1/3} C^{2/3}$. For brevity, we denote the term $|\dot{x}\ddot{y} - \ddot{x}\dot{y}|$ as D (same notation as in M/S):

$$A = D^{1/3} C^{2/3} \tag{6}$$

or equivalently $V = D^{1/3} C^{-1/3}$. In logarithmic units, $\log A = \frac{1}{3}\log D + \frac{2}{3}\log C$ or $\log V = \frac{1}{3}\log D - \frac{1}{3}\log C$. Notice that, in Eq. 6, D depends simultaneously on both speed and curvature. In fact, using the formulas by de L'Hôpital and Faà di Bruno, we can rewrite:

$$\dot{x}\ddot{y} - \ddot{x}\dot{y} = \frac{dx}{ds}\frac{ds}{dt}\frac{d^2y}{dt^2} - \frac{dy}{ds}\frac{ds}{dt}\frac{d^2x}{dt^2} = \left(\frac{ds}{dt}\right)^3 \left(\frac{dx}{ds}\frac{d^2y}{ds^2} - \frac{dy}{ds}\frac{d^2x}{ds^2}\right) \tag{7}$$

Equation 7 makes explicit the simultaneous dependence of D on speed and curvature, since the term $\left(\frac{ds}{dt}\right)^3$ is the third power of the tangential speed, while the term $\left(\frac{dx}{ds}\frac{d^2y}{ds^2} - \frac{dy}{ds}\frac{d^2x}{ds^2}\right)$ is the curvature.

Therefore, Eq. 6 represents a simple mathematical identity and does not imply that A depends on two independent variables, D and C, because in the absence of constraints A and V remain mathematically independent of C and R. Moreover, D cannot be considered an independent predictor of V (or A) because D itself depends on V (or A).

For an arbitrary motion, in Eq. 6, A, D and C are all time-varying functions along the traced curve. However, in the special case in which D does not vary with time throughout the movement, that is, when $D^{1/3} = K =$ constant, Eq. 6 satisfies Eq. 1 with a power exponent of β exactly equal to 2/3. In other words, the special condition of $D^{1/3} = K$ yields the 2/3 power law for the speed-curvature consistently found for elliptic drawings (see above). In the following, we will consider conditions that either satisfy or violate $D^{1/3} =$ constant. First, we describe mathematical and physical examples, and then we consider biological constraints that result in a nearly constant value of $D^{1/3}$.

The power law is not obligatory mathematically

Before we have used formal arguments to show that a given path of movement can be traced with different speed profiles, since the path specifies the instantaneous movement direction but not the speed. In this section we provide analytical and numerical calculations to demonstrate the same fact. To this end, we use the prototypical case of an elliptic path that, when drawn by humans or monkeys, typically complies with the 2/3 power law. In our simulations, the geometry of the curve is constant, while the kinematics is specified by means of the usual parametric representation in sine and cosine functions of the angle θ_t. However, we define different time profiles for θ_t, with the result of obtaining for the same geometry different kinematics, and therefore different relationships between angular speed and curvature.

Methods and results

Figure 4 shows the results of three different simulations of elliptic motion. We present both the analytical solutions and the results of numerical calculations (Fig. 4d). For the latter, the time-discrete trajectories were interpolated (cubic splines) to obtain first and second time derivatives, which were then used to calculate curvature C and angular speed A.

In all three simulations, the kinematics is defined by the equations:

$$x = a\sin\left(2\pi\theta_t\right), y = b\cos\left(2\pi\theta_t\right) \tag{8}$$

Only in the first simulation (top panel, Fig. 4b) does the angle θ_t have a simple, linear dependence on time ($\theta_t = t$). In the other two cases, θ_t has a more complex, non-linear time-dependence (middle and bottom, Fig. 4b). In particular, the target slows down as curvature increases (toward the vertices), progressively accelerates, and slows down as curvature decreases, in the first, second and third simulation, respectively. As a result, the angular speed A and curvature C co-vary throughout the movement in the first case (top, Fig. 4c), whereas the relationship between A and C changes over one cycle for the other two cases (middle and bottom, Fig. 4c). Accordingly, log$A$ is linearly related to log$C$ with an exponent β equal to 2/3 in the first case (top, Fig. 4d), whereas the relationship log$A$ versus log$C$ is complex and the 2/3 power law is violated in the other two cases (middle and bottom, Fig. 4d).

To see why this happens, we remind that the critical condition to satisfy exactly the 2/3 power law is given by $D = |\dot{x}\ddot{y} - \ddot{x}\dot{y}| =$ constant. By taking the time derivatives of Eq. 8 and performing straightforward calculations, we find that $D = ab\left(2\pi\left|\dot{\theta}\right|\right)^3$. Now, for the first case we considered ($\theta_t = t$), we find that $D = ab(2\pi)^3 =$ constant, and $A = KC^{2/3}$ is satisfied exactly. In fact, the notion that orthogonal harmonic oscillations (such as those of Eq. 8 with $\theta_t = t$) generate motions that comply with the 2/3 power law has long been established (Lacquaniti et al. 1983). Notice further that, if we scale up the motion speed by a constant ($\theta_t = ct$), then D scales up with c^3 and the 2/3 power law still holds but the A–C curve is shifted upwards, consistent with the published results of the effects of changes in average speed of human hand-drawing (Lacquaniti et al. 1983). In contrast with the previous cases, in the elliptic trajectories in which θ_t has a non-linear time-dependence (as in the second and

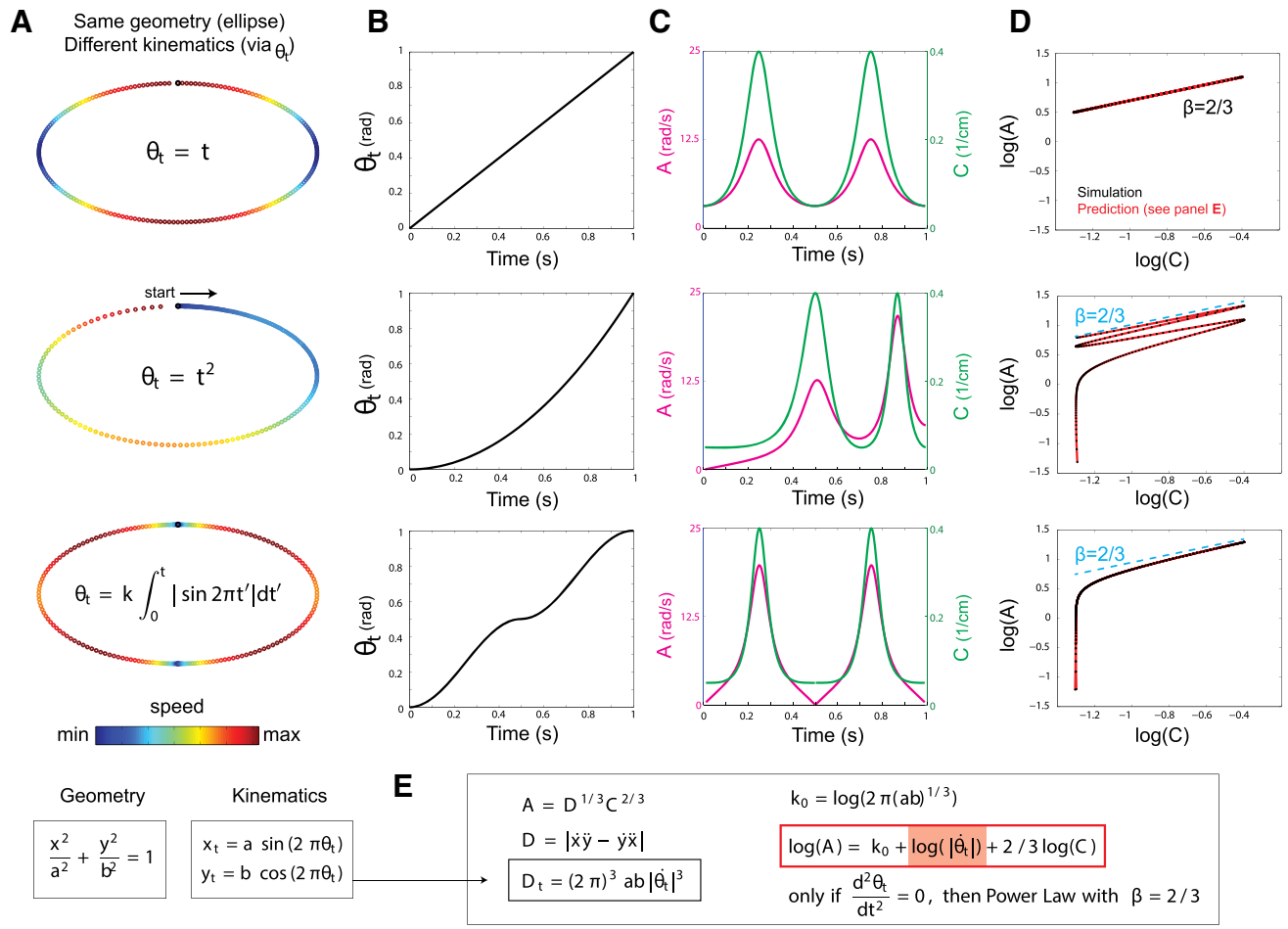

Fig. 4 Mathematical models and numerical simulations of one ellipse traced with three different kinematics (top, middle, bottom row). **a** Each point of the ellipses is colored according to the instantaneous tangential speed. The defining equations for the angles θ_t are in the insets. The moving point slows down with increasing curvature, progressively accelerates over one cycle, and slows down with decreasing curvature in the top, middle and bottom panels, respectively. The bottom inset reports the general parametric equations for the geometry and kinematics of the ellipses, with $a = 10$, $b = 5$ cm. **b** Time course of θ_t for the three kinematic cases depicted in (A) over one cycle. **c** The corresponding time profiles of angular speed A (magenta) and curvature C (green). **d** Log–log plots of A and C, for both the analytical (red) and the numerical (black) solutions. For comparison, blue dashed lines with 2/3 slope are shown in the middle and bottom panels. **e** Summary of the main mathematical expressions for the speed-curvature relation of ellipses traced with different kinematics

third simulations of Fig. 4), D is not constant any more but changes drastically (with the 3rd power of the rate of change of the angle θ_t). Therefore, in all such cases, the 2/3 power law is mathematically violated.

The power law is not obligatory in physical systems

In this section, we address another theoretical issue about the nature of the speed-curvature power-law: Does any object obey necessarily the law irrespective of the underlying forces because of the way the law is derived? If this were the case, we should be able to derive the law also for the motion of any arbitrary, inanimate body subjected to non-biological forces. In the following, we provide examples of the motion of objects affected by gravitational, drag or elastic forces, and we show that most of them violate the speed-curvature power law, while one example complies with the law.

Methods and results

Figures 5a–d show the results of simulations of a few different systems whose kinematics is dictated by the dynamic equations provided in Fig. 5e. In all cases, the dynamic equations of motion were numerically integrated by means of time-step Euler integration. The time-discrete, unfiltered trajectories were interpolated (cubic splines) to obtain first and

second time derivatives, which were then used to calculate curvature and angular speed.

The first physical system we consider is given by an ideal binary star consisting of two bodies of equal mass, under Newton's law of universal gravitation (Fig. 5a). The gravitational pull between the two bodies causes them to move in elliptic orbits around their common center of mass. Unsurprisingly, we find that the instantaneous angular speed of each body can be either very large or very small for the same values of local curvature. The log–log plot of angular speed and curvature shows that the power law is clearly violated. Once more, the result can be predicted by considering that $D = |\dot{x}\ddot{y} - \ddot{x}\dot{y}|$ is not constant for this system (Fig. 5e). Similar results are obtained (data not shown) when we consider the case where one body is massive, such as the Sun, and the other one is much less massive, such as a planet orbiting around the Sun. We then rediscover Kepler's observation that in perihelion (the point closest to the Sun) the planet is moving faster than in aphelion (the point farthest from the Sun). Since these two points have the same curvature, it is clear that speed and curvature do not co-vary, violating the power-law.

The second physical system consists of a projectile launched in ballistic trajectory under the action of gravity (Fig. 5b). We consider two cases, namely that the projectile motion is affected (thin line) or unaffected (thick line) by a drag force proportional to speed. Without drag, angular speed and curvature co-vary, and the 2/3 power law is obeyed. With drag, instead, the law is violated. In fact, by considering the corresponding dynamic equations (Fig. 5e), we see that D is constant without drag, but is non-constant with linear drag. Notice that D is non-constant also with quadratic drag (valid at high speeds): $D = \left|-g\dot{x} - k(\dot{x}\dot{y}^2 - \dot{y}\dot{x}^2)\right|$.

The third physical system is a simple pendulum under gravity, without drag (Fig. 5c). This system provides a dramatic violation of the speed-curvature power-law (La Scaleia et al. 2014). The oscillations of the pendulum trace a circle and thus curvature is constant throughout, while angular speed changes throughout, being zero at the extremes of the swing and maximal in the middle point. Accordingly, the log–log plot of angular speed vs. curvature yields a line parallel to the ordinates axis.

Finally, we consider a system consisting of a mass connected to two orthogonal linear springs, whose elastic force is proportional to the distance from equilibrium length (Fig. 5d). Depending on the initial conditions and parameter values, speed and curvature can approximate a power law, but in general the power law is not obeyed exactly.

Different biological constraints may give rise to the speed-curvature power law

We have previously argued that the power law is not a trivial relationship given by mathematics or physics. Here we consider a number of potential physiological constraints that may underlie non-trivial speed-curvature power laws found in empirical studies of biological movements. One approach consists in investigating specific kinematic conditions under which D in Eq. 6 is constant or nearly constant, thus yielding speed-curvature relationships closely obeying the 2/3 power law. As we mentioned above, Lacquaniti et al. (1983) showed that orthogonal harmonic oscillations at the same frequency generate 2D elliptic drawings that always comply with the 2/3 power and, for such condition, D in Eq. 6 is exactly constant.[3] Even in the case of harmonic oscillations that are not orthogonal, such as those generated by coupled angular motions at the limb joints, D can vary little with time. Thus, Soechting and Terzuolo (1986) and Schaal and Sternad (2001) showed that, for periodic drawings of ellipses in 3D, the condition $D \approx$ constant is satisfied by sinusoidal motion of the limb segments with appropriate inter-segmental phase shifts. Dounskaia (2007) elaborated further on the implications of sinusoidal angular motions using a simplified model of planar 2D drawing movements. She showed that the condition $D^{1/3} \approx$ constant holds when the shoulder and elbow perform sinusoidal angular motions of moderate amplitudes with a substantial phase offset, whereas the condition is violated ($D^{1/3}$ widely time-varying) when the angular motions are very large or very small (consistent with previous experimental observations by Wann et al. 1988 and Schaal and Sternad 2001).

However, only some biological movements are subserved by simple sinusoidal motions. For instance, the small hand drawing movements of the convex curves that we described earlier (see Empirical speed-curvature power laws for human drawing have different exponents) involve important contributions by wrist and fingers (in addition to shoulder and elbow), which exhibit considerable harmonic distortion and whose phase is quite variable (Lacquaniti et al. 1987). Since the different convex curves of Fig. 2 (as well as those of Huh and Sejnowski 2015) were all of about the same size and were performed at about the same average speed, the different values of the exponent β as a function of curve shape cannot be explained on the basis of the average speed and amplitude of oscillation at the shoulder and elbow joints (Dounskaia 2007).

[3] Notice, however, that orthogonal harmonic oscillations at a different frequency generate Lissajous motions that do not comply necessarily with the 2/3 power law (Lebedev et al. 2001).

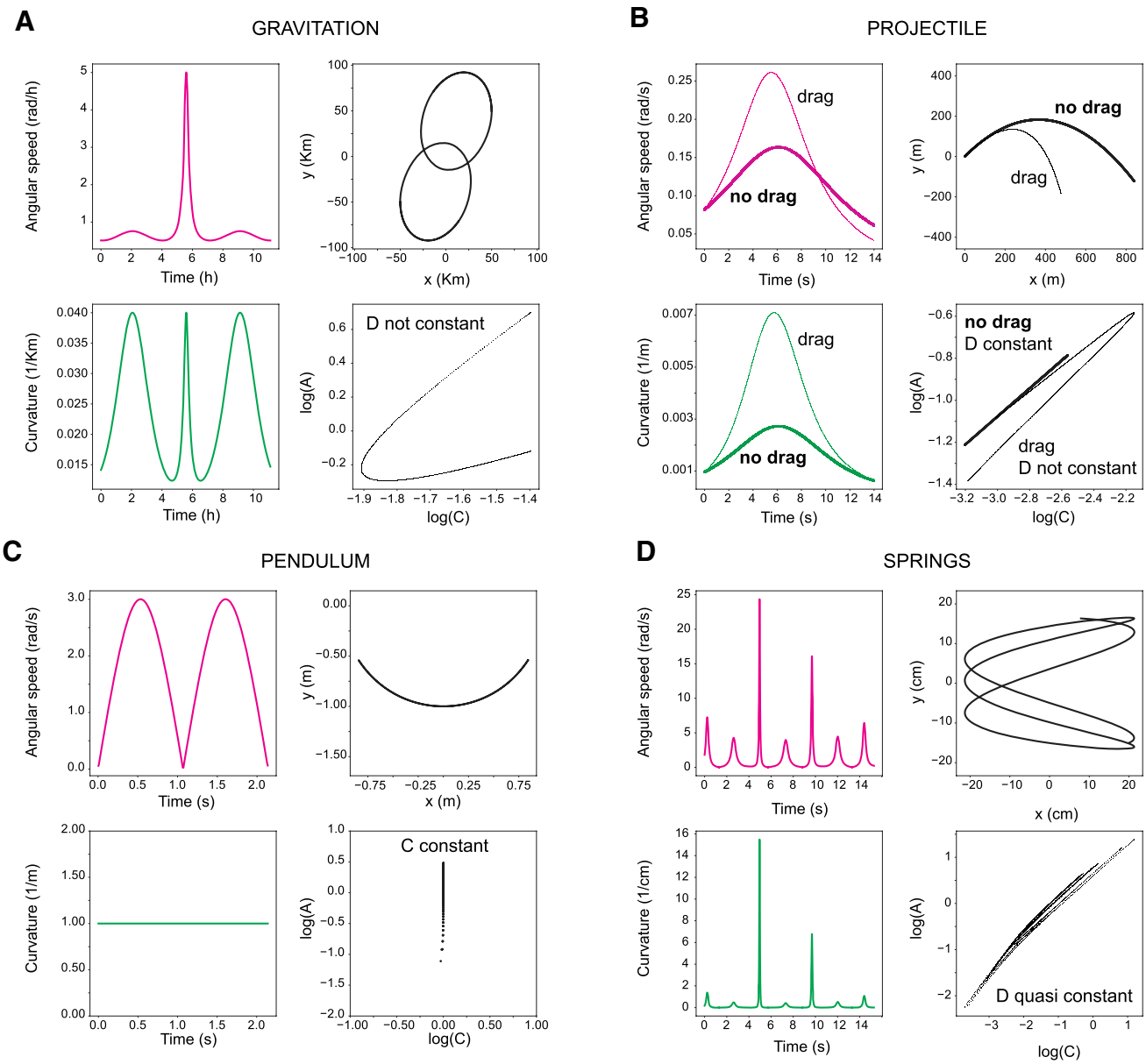

E

GRAVITATION

$$\ddot{x}_1 = -k(x_1 - x_2)/r^3$$
$$\ddot{y}_1 = -k(y_1 - y_2)/r^3$$

$$D = |\dot{x}\ddot{y} - \dot{y}\ddot{x}| \neq \text{constant}$$

PROJECTILE

$$\ddot{x} = -k\dot{x}$$
$$\ddot{y} = -g - k\dot{y}$$

$$D_{k=0} = |0 + g\dot{x}| = |gv_0| = \text{constant}$$
(no drag)

PENDULUM

$$\ddot{\theta} = -(g/L)\sin\theta$$
$$x = L\sin(\theta)$$
$$y = -L\cos(\theta)$$

$$D = L^2|\dot{\theta}|^3 \quad \text{so} \quad C = 1/L = \text{constant}$$

SPRINGS

$$\ddot{x} = -k_x x$$
$$\ddot{y} = -k_y y$$

$$D = |k_x x\dot{y} - k_y y\dot{x}| \simeq \text{constant}$$

◂**Fig. 5** Physical models and numerical simulations of the kinematics of different systems subject to gravitational, drag or elastic forces. **a** Two gravitating bodies of equal mass, such as two equal stars orbiting around their common barycenter. **b** Ballistic projectiles thrown with an initial speed and accelerated downwards by gravity in the presence (thin lines) or absence (thick lines) of drag. **c** Simple pendulum accelerated by gravity in the absence of drag. **d** Two uncoupled linear springs. Subpanels in A–D show in clockwise order: angular speed (magenta) versus time, x coordinate versus y coordinate of the moving object, log–log plot of angular speed and curvature, and curvature (green) versus time. **e** Differential equations used to simulate the different physical systems, together with the analytical assessment of whether or not the term D = constant and the 2/3 power law is satisfied. Parameters are: $k = 0.04$, r = instantaneous distance between the two bodies for gravitation; $k = 0.09$ and $g = 9.81$ m s^{-2} for the projectiles; $L = 1$ m and $g = 9.81$ m s^{-2} for the pendulum; $k_x = 1.78$ and $k_y = 0.33$ s^{-2} for the springs

A different perspective on the significance of the constraint was brought up by consideration of the geometrical structure of the internal representations of human movements and perceptions (Pollick and Sapiro 1997; Flash and Handzel 2007; Polyakov et al. 2009; Bennequin et al. 2009). Although Euclidean geometrical representations are often assumed, there is growing evidence that both movement planning and visual perception may rely on representations drastically departing from Euclidean geometry, such as affine and equi-affine geometries (Koenderink and van Doorn 1991; Bennequin et al. 2009). Following this approach, Pollick and Sapiro (1997) and Flash and Handzel (2007) showed that $D^{1/3}$ = constant implies that the equi-affine speed V_{ea} is constant, since $V_{ea} = |\dot{x}\ddot{y} - \ddot{x}\dot{y}|^{1/3}$ (Guggenheimer 1977). Therefore, the 2/3 power law is predicted by assuming a constant equi-affine speed throughout the movement. On the other hand, a combination of Euclidean, affine, and equiaffine geometries can generate variable power law exponents, depending on the shape of the trajectory, consistent with the observations by Huh and Sejnowski (2015), replicated in our earlier section of this article.

Still a different approach relies on the assumption that the motor system optimizes a given cost function along the trajectory. In particular, the minimum-jerk model has frequently been associated with the speed-curvature power law (Wann et al. 1988; Viviani and Flash 1995; Todorov and Jordan 1998; Richardson and Flash 2002; Huh and Sejnowski 2015). This model assumes the minimization of squared hand jerk (the rate of change of acceleration) summed over movement duration T: $\int_0^T (\dddot{x}^2 + \dddot{y}^2)dt$. Todorov and Jordan (1998) argued that the constraint of the 2/3 power law provides an efficient solution to the minimization of the total jerk along a prescribed trajectory, since it sets the normal component of jerk to zero. Indeed, by taking time derivatives and canceling terms, the expression $\dot{x}\ddot{y} - \ddot{x}\dot{y}$ = constant is shown to be equivalent to $\frac{\dot{x}}{\dot{y}} = \frac{\ddot{x}}{\ddot{y}}$, which implies that the jerk vector should be parallel to the tangential velocity vector, so that the jerk component in the normal direction is zero (Soechting and Terzuolo 1986; Todorov and Jordan 1998). Huh and Sejnowski (2015) expressed the total squared-jerk cost to be minimized in the Frenet–Serret moving frame. Remarkably, this model revealed scale-invariant features of 2D curved movements and accounted for a spectrum of power laws with a wide range of exponents for different pure frequency curves (see above), as well as for mixtures of power laws for multi-frequency curves such as those associated with scribbling. This approach is related to the Cartan's moving frame method used by Bennequin et al. (2009), which also predicts a mixture of geometries compatible with a spectrum of power exponents, not just the 2/3 power exponent. Lebedev et al. (2001) argued instead that the 2/3 power law arises from the principle of least action; viz. if a movement between two points of a given path obeys the 2/3 power law, then the amount of work required to execute a trajectory in a fixed time is minimal. In fact, the principle of least action states that the integral $\int_0^T \dot{x}^3(\frac{d^2y}{dx^2})dt$ must be minimal over movement duration T, and this condition is satisfied when $\dot{x}^3\left(\frac{d^2y}{dx^2}\right)$ = constant. Since $\dot{x}\ddot{y} - \ddot{x}\dot{y} = \dot{x}^3(\frac{d^2y}{dx^2})$, it follows that a movement obeying the 2/3 power law satisfies the principle of least action (Lebedev et al. 2001).

Omitted variable bias hypothesis

M/S argue that the Equation $A \approx KC^{\beta}$ (Eq. 1) and the equivalent ones (Eqs. 2–4) typically used to assess speed-curvature relationships in biological movements are inappropriate, because these equations omit the predictor variable $D^{1/3}$ that is included in the expression $A = D^{1/3}C^{2/3}$ (Eq. 6). However, this argument is flawed since D of Eq. 6 is not an independent variable, but depends on both A and C (or V and R), as we showed in an earlier section (A different way to look at speed-curvature relationships). Therefore, D cannot be considered an independent predictor of A (or V), because D itself depends on A (or V). If one applied to experimental data a statistical regression based on Eq. 6 (as M/S do), one would learn nothing at all about the physiological underpinnings of the relationship between speed and curvature, because Eq. 6 is a mathematical identity that must always be satisfied, apart from measurement errors. In fact, the only interest in performing a statistical regression on Eq. 6 (or its log–log equivalent) would lie in the study of noise effects (see below). This is acknowledged by M/S when they state that a statistical regression analysis that included $D^{1/3}$ as a predictor variable would always find the exponent of C in Eq. 6 to be exactly equal to its true value 2/3. Accordingly, their application of the principles of omitted variable bias

(OVB, see Wooldridge 2012) to the speed-curvature relationship is ill-grounded, since OVB applies to linear regressions of a dependent variable on one or more independent variables, and here C is an independent variable but D is not.

Given the circularity of M/S argument based on a mathematical identity, it is totally unsurprising that M/S are able to calculate the value of the deviation of the exponent β of Eq. 1 from the 2/3 value based on Eq. 6. Indeed, this had already been shown by Maoz et al. (2006), who performed the statistical regressions to show the potential effects of measurement noise. Maoz et al. (2006) showed that, if one considers all variables as random variables affected by measurement noise, $A = D^{1/3}C^{2/3}$ (Eq. 6) implies that $\beta = \frac{2}{3} + \frac{\xi}{3}$, where β denotes the linear regression coefficient of log$A$ versus log$C$ and ξ denotes the linear regression coefficient of log$D$ versus log$C$. In turn, $\xi = \frac{\mathrm{Cov}(\log C, \log D)}{\mathrm{Var}(\log C)}$ where Cov and Var are the covariance and variance of the indicated variables. Therefore, if log$D$ and log$C$ (as derived from experimental measurements) are statistically uncorrelated, $Cov(\log C, \log D) = 0$, $\xi = 0$ and $\beta = 2/3$, thus fulfilling exactly the 2/3 power law. For all other cases, instead, $Cov(\log C, \log D) \neq 0$, $\xi \neq 0$ and $\beta \neq 2/3$. Therefore, the experimental finding of a range of β values (including the special case of $\beta = 2/3$) for different kinds of biological movements implies that the control systems are able of establishing non-trivial co-regulations of path geometry and kinematics.

As we discussed at length before (see Different biological constraints may give rise to the speed-curvature power law), D is not a predictor variable but its behavior, whether it is nearly constant or widely time-varying throughout a movement, can tell us something about the physiological mechanisms underlying the generation of a given biological movement (Lacquaniti et al. 1983; Soechting and Terzuolo 1986; Viviani and Flash 1995; Pollick and Sapiro 1997; Todorov and Jordan 1998; Maoz et al. 2006; Dounskaia 2007; Flash and Handzel 2007; Polyakov et al. 2009; Bennequin et al. 2009). Interestingly, the message stemming from these previous studies goes in the opposite direction to that of M/S. Rather than being mathematical/statistical artifacts, empirical speed-curvature power laws are real and require a critical investigation of the properties of D to account for compliance or deviation of empirical β values relative to the prototypical 2/3 value found in elliptic drawings, and to test different hypotheses about the physiological origin of the speed-curvature relationships.

Real statistical issues with the power law analysis

A general caveat is that caution is necessary before claiming that experimental measurements conform to a power law, unless a mechanistic model of the system dynamics specifically predicts such a law (Stumpf and Porter 2012). In theory, a power law should be scale invariant, that is, the functional relationship between the two variables should be independent of their magnitude. In practice, few empirical phenomena obey power laws for all values of the variables, and therefore the corresponding law should be defined only over a specified domain.

Statistical support for a power law is often searched using log–log plots, given the simplicity of this analysis (the exponent of the law being found by linear regression). This is also the case for most studies of the speed-curvature power law. A common rule of thumb to assess a candidate power law is that it should exhibit an approximately linear relationship on a log–log plot over at least two orders of magnitude in both the x and y axes (Stumpf and Porter 2012). For instance, Fig. 3 shows that the log–log regressions of speed versus curvature for the experimental data with crawling larvae comply with this criterion (see also Zago et al. 2016). When this criterion is not fulfilled, there are additional statistical tests that can be used to validate power law distributions (Clauset et al. 2009).

One drawback of using log–log regressions is that they tend to de-emphasize the error of data points at the higher ends of the range of values, i.e. higher speeds and curvatures in the present case. Schaal and Sternad (2001) compared log–log regressions and nonlinear regressions of speed versus curvature for drawing of ellipses in 3D space, and found that log–log regressions slightly but systematically underestimated the absolute deviations from the coefficient expected from the 2/3 power law. Therefore, when high speeds and curvatures are important for a specific study, nonlinear regressions should be used instead of log–log regressions.

Correlation versus causation

In several experiments dealing with the speed-curvature power law, the path was unconstrained, so that both instantaneous curvature and speed can vary freely, and indeed the point of the law is that their changes are tightly correlated (coupled) between each other. On the other hand, it is incorrect to state that "Since neither of these variables [i.e., curvature or speed, our note] is manipulated under controlled conditions, any observed relationship between them cannot be considered to be causal" (M/S, pg. 1836). In fact, in a series of previous experiments, movement was guided by asking participants to follow with the pen tip the inner edge of a Plexiglas template cut by a numerical control milling machine (Lacquaniti et al. 1983; Catavitello et al. 2016). Each template resembled an ellipse but consisted of two pairs of circular arcs with different radii. A set of 11 such templates was built by varying the radii so that the shape of

the templates varied progressively from a circle to a very elongated pseudo-ellipsis, while the perimeter was kept constant. This step-response paradigm allowed to address the relation between the geometry of the trajectory and the speed of execution in a controlled manner. Recordings from each template resulted in a pair of data points in the log angular speed versus log curvature plot, one for the more curved and the other one for the less curved portions of the trajectory. All data points were well fitted by power functions, but the power exponents decreased with increasing average speed of execution (Fig. 4 in Lacquaniti et al. 1983). Using the same templates, Catavitello et al. (2016) investigated the speed changes occurring at the transitions between the two circular arcs and found that they occurred before the radius changed from large to small, possibly reflecting an anticipatory control of path trajectory (Tramper and Flanders 2013), but the reverse transition (small to large radius) did not involve a similar anticipation. Several other studies have explored the manual tracing of template figures, thus manipulating curvature under controlled conditions (e.g., Wann et al. 1988; Viviani and Flash 1995; Todorov and Jordan 1998; Richardson and Flash 2002; Flash and Handzel 2007; Huh and Sejnowski 2015).

On a theoretical basis, the causal relationship between curvature and speed is predicted by models assuming that the geometrical shape of a given movement is pre-planned while the speed profile results from movement optimization (Wann et al. 1988; Viviani and Flash 1995; Todorov and Jordan 1998; Richardson and Flash 2002; Flash and Handzel 2007; Huh and Sejnowski 2015) or non-Euclidean implementations of the plan (Pollick and Sapiro 1997; Flash and Handzel 2007; Polyakov et al. 2009; Bennequin et al. 2009). Specifically, Huh and Sejnowksi (2015) showed that movement speed depends not only on the instantaneous curvature, but also on the nearby curvature within 1 rad of the angle coordinate α, suggesting that the angle coordinate and therefore curvature only need to be planned 1 rad ahead. This is consistent with the result of Tramper and Flanders (2013) that planning (or anticipation) takes over longer distance and time when the radius changes from large to small, and shorter distance and time when the radius changes from small to large.

M/S rightly point out that "muscle forces will not be consistently related to the curvature and velocity of the movement" (pg. 1836). Indeed, it has been long known that the changes in electrical muscle activity (EMG) and joint torques follow a time course different from that of hand or joint kinematics. For instance, drawing of ellipses in 3D tends to comply with the 2/3 power law and involves sinusoidal angular motions at the shoulder and elbow joints (Soechting et al. 1986; Schaal and Sternad 2001). Instead the corresponding joint torques and EMG activities deviate substantially from sinewaves (Soechting et al. 1986). The relationship between neural commands, muscle forces, joint torques, and hand kinematics is very complex, being stochastic, non-linear, and closed-loop. For instance, due to the existence of sensory feedbacks with substantial time delays, the muscle forces do not simply affect movement output, but in turn they are affected by the movement via the feedback loops. Therefore, the inference drawn by M/S that "An alternative to a causal explanation of the power law is that the law is an inherent characteristic of the mathematical relationship between measures of curvature and velocity obtained during any curved movement" (pg. 1836) is logically a non sequitur, given the complex relationship between muscle forces and movement kinematics.

Conclusion

Although some of the arguments and simulations we presented probably appear trivial to mathematically oriented readers, they are important to be clarified since illusory issues are still lingering around the speed-curvature power law, as demonstrated by M/S paper. We believe that our analyses are sufficient to refute the argument that "the power law of movement is an observation forced by the mathematical relationship between measures of the curvature and velocity of movement that are used in power law research" (M/S, pg. 1841).

Contrary to M/S conclusion, we maintain that the speed-curvature power law is real and it applies to a wide variety of biological movements with different values of the exponent. The issue that remains to be solved concerns the physiological origins of the power law. But this is a different topic to be covered in a forthcoming article.

Acknowledgements The authors declare no competing financial interests. The work was supported by the Italian Space Agency (grant n. I/006/06/0 to F.L. and grant n. 2014-008-R.0 to M.Z.), the Italian University Ministry (PRIN grant 2015HFWRYY_002 to F.L.), the Spanish Ministry of Economy and the Severo Ochoa Center of Excellence programs (SEV-2013-0317 start-up funds to A.G.-M., grant BFU-2015-74241-JIN to A.G.-M., and pre-doctoral contract BES-2016-077608 to A.M.). Tamar Flash is an incumbent of Dr. Haim Moross professorial chair. The funders had no role in study design, data collection and analysis, decision to publish, or preparation of the manuscript. We thank the anonymous reviewers for helpful suggestions.

References

Abeles M, Diesmann M, Flash T, Geisel T, Herrmann M, Teicher M (2013) Compositionality in neural control: an interdisciplinary study of scribbling movements in primates. Front Comput Neurosci 7:103. doi:10.3389/fncom.2013.00103

Bennequin D, Fuchs R, Berthoz A, Flash T (2009) Movement timing and invariance arise from several geometries. PLoS Comput Biol 5(7):e1000426

Catavitello G, Ivanenko YP, Lacquaniti F, Viviani P (2016) Drawing ellipses in water: evidence for dynamic constraints in the relation between speed and path curvature. Exp Brain Res 234:1649–1657
Clauset A, Shalizi CR, Newman ME (2009) Power-law distributions in empirical data. SIAM Rev 51(4):661–703
de'Sperati C, Viviani P (1997) The relationship between curvature and speed in two-dimensional smooth pursuit eye movements. J Neurosci 17:3932–3945
Dounskaia N (2007) Kinematic invariants during cyclical arm movements. Biol Cybern 96:147–163
Flanders M, Mrotek LA, Gielen CC (2006) Planning and drawing complex shapes. Exp Brain Res 171:116–128
Flash T, Handzel AA (2007) Affine differential geometry analysis of human arm movements. Biol Cybern 96:577–601
Gielen CC, Dijkstra TM, Roozen IJ, Welten J (2009) Coordination of gaze and hand movements for tracking and tracing in 3D. Cortex 45:340–355
Gomez-Marin A, Stephens GJ, Louis M (2011) Active sampling and decision making in Drosophila chemotaxis. Nat Commun 2:441
Gomez-Marin A, Partoune N, Stephens GJ, Louis M (2012) Automated tracking of animal posture and movement during exploration and sensory orientation behaviors. PLoS One 7:e41642
Gribble PL, Ostry DJ (1996) Origins of the power law relation between movement speed and curvature: modeling the effects of muscle mechanics and limb dynamics. J Neurophysiol 76:2853–2860
Guggenheimer HW (1977) Differential geometry. Dover, New York, p 378
Harris CM, Wolpert DM (1998) Signal-dependent noise determines motor planning. Nature 394:780–784
Hicheur H, Vieilledent S, Richardson MJE, Flash T, Berthoz A (2005) Speed and curvature in human locomotion along complex curved paths: a comparison with hand movements. Exp Brain Res 162:145–154
Huh D (2015) The vector space of convex curves: how to mix shapes. arXiv:1506.07515
Huh D, Sejnowski TJ (2015) Spectrum of power laws for curved hand movements. Proc Natl Acad Sci 112:E3950–E3958
Ivanenko YP, Grasso R, Macellari V, Lacquaniti F (2002) Two-thirds power law in human locomotion: role of ground contact forces. NeuroReport 13:1171–1174
Koenderink JJ, van Doorn AJ (1991) Affine structure from motion. J Opt Soc Am A 8:377–385
La Scaleia B, Zago M, Moscatelli A, Lacquaniti F, Viviani P (2014) Implied dynamics biases the visual perception of speed. PLoS One 9(3):e93020
Lacquaniti F, Terzuolo C, Viviani P (1983) The law relating the kinematic and figural aspects of drawing movements. Acta Psychol (Amst) 54:115–130
Lacquaniti F, Terzuolo C, Viviani P (1984) Global metric properties and preparatory processes in drawing movements. In: Kornblum S, Requin J (eds) Preparatory states and processes. Erlbaum, Hillsdale, pp 357–370
Lacquaniti F, Ferrigno G, Pedotti A, Soechting JF, Terzuolo C (1987) Changes in spatial scale in drawing and handwriting: kinematic contributions by proximal and distal joints. J Neurosci 7:819–828
Lebedev S, Tsui WH, Van Gelder P (2001) Drawing movements as an outcome of the principle of least action. J Math Psychol 45:43–52
Maoz U, Portugaly E, Flash T, Weiss Y (2006) Noise and the 2/3 power law. Adv Neural Inf Proc Syst 18:851–858
Maoz U, Berthoz A, Flash T (2009) Complex unconstrained three-dimensional hand movement and constant equi-affine speed. J Neurophysiol 101:1002–1015
Marken RS, Shaffer DM (2017) The power law of movement: an example of a behavioral illusion. Exp Brain Res 235:1835–1842
Massey JT, Lurito JT, Pellizzer G, Georgopoulos AP (1992) Three-dimensional drawings in isometric conditions: relation between geometry and kinematics. Exp Brain Res 88:685–690
Pollick FE, Sapiro G (1997) Constant affine speed predicts the 1/3 power law of planar motion perception and generation. Vision Res 37:347–353
Pollick FE, Maoz U, Handzel AA, Giblin P, Sapiro G, Flash T (2009) Three-dimensional arm movements at constant equi-affine speed. Cortex 45:325–339
Polyakov F, Stark E, Drori R, Abeles M, Flash T (2009) Parabolic movement primitives and cortical states: merging optimality with geometric invariance. Biol Cybern 100:159–184
Richardson MJE, Flash T (2002) Comparing smooth arm movements with the 2/3 power law and the related segmented-control hypothesis. J Neurosci 22:8201–8211
Schaal S, Sternad D (2001) Origins and violations of the 2/3 power law in rhythmic three-dimensional arm movements. Exp Brain Res 136:60–72
Schwartz AB (1994) Direct cortical representation of drawing. Science 265:540–542
Soechting JF, Terzuolo CA (1986) An algorithm for the generation of curvilinear wrist motion in an arbitrary plane in three-dimensional space. Neuroscience 19:1393–1405
Soechting JF, Lacquaniti F, Terzuolo CA (1986) Coordination of arm movements in three-dimensional space. Sensorimotor mapping during drawing movement. Neuroscience 17:295–311
Struik DJ (2012) Lectures on classical differential geometry. Dover Publ, New York
Stumpf MP, Porter MA (2012) Critical truths about power laws. Science 335:665–666
Todorov E, Jordan MI (1998) Smoothness maximization along a predefined path accurately predicts the speed profiles of complex arm movements. J Neurophysiol 80:696–714
Tramper JJ, Flanders M (2013) Predictive mechanisms in the control of contour following. Exp Brain Res 227:535–546
Vieilledent S, Kerlirzin Y, Dalbera S, Berthoz A (2001) Relationship between speed and curvature of a human locomotor trajectory. Neurosci Lett 305:65–69
Viviani P, Cenzato M (1985) Segmentation and coupling in complex movements. J Exp Psychol Hum Percept Perform 11:828–845
Viviani P, Flash T (1995) Minimum-jerk, 2/3 power law, and isochrony: converging approaches to movement planning. J Exp Psychol Hum Percept Perform 21:32–53
Viviani P, Schneider R (1991) A developmental study of the relationship between geometry and kinematics in drawing movements. J Exp Psychol Hum Percept Perform 17:198–218
Viviani P, Terzuolo C (1982) Trajectory determines movement dynamics. Neuroscience 7:431–437
Wann J, Nimmo-Smith I, Wing AM (1988) Relation between speed and curvature in movement: equivalence and divergence between a power law and a minimum-jerk model. J Exp Psychol Hum Percept Perform 14:622–637
West G (2017) Scale. Penguin, New York, p 479
Wolpert DM, Pearson KG, Ghez CPJ (2013) The organization and planning of movement. Princ Neural Sci 5:743–766
Wooldridge JM (2012) Introductory econometrics: a modern approach. South-Western Cengage Learning, Mason, pp 88–93
Zago M, Lacquaniti F, Gomez-Marin A (2016) The speed-curvature power law in *Drosophila* larval locomotion. Biol Lett 12(10):20160597